902 *Organometallics* **1998,** *17,* 902−907

Metallaborane Heteroatom Incorporation Reactions: Enyne Insertion into *arachno*-$[(CO)(PMe_3)_2HIrB_8H_{12}]$

Jonathan Bould,[†,‡] Nigam P. Rath,[‡] Lawrence Barton,[‡] and John D. Kennedy[†]

The School of Chemistry, University of Leeds, Leeds LS2 9JT, England, and Department of Chemistry, University of Missouri−St. Louis, St. Louis, Missouri 63121

Received July 31, 1997

arachno-$[(CO)(PMe_3)_2HIrB_8H_{12}]$ (**1**) reacts with $HC{\equiv}C{-}C(CH_3){=}CH_2$ in xylene at 138 °C to afford $[7\text{-}\{C(CH_3)CH_2\}\text{-}9,9,9\text{-}(CO)(PMe_3)_2$-*nido*-$9,7,8\text{-}IrC_2B_8H_{10}]$ (**2**; 10%) together with traces of $[5,5,5\text{-}(CO)(PMe_3)_2\text{-}\mu\text{-}6,7\text{-}\{CHC(CH_3)CH_2\}$-*nido*-$5,6\text{-}IrCB_8H_{11}]$ (**3**, <1%). Compound **2** is a conventional *nido* 11-vertex metallacarborane with the $\{C_2Ir\}$ three-atom string in the open face of the cluster, whereas compound **3** is based on a *nido* 10-vertex $\{5,6\text{-}IrCB_8\}$ skeleton with C(2) of the original butyne bridging adjacent B(7) and C(6) cluster open-face positions. Compounds **2** and **3** are characterized by ^1H, ^{31}P, and ^{11}B NMR spectroscopy and by single-crystal X-ray diffraction analysis.

Introduction

Metallaborane cage chemistry is an interesting and increasingly developing field of study.[1] However, particularly because of the large variety of novel structural motifs that are continually revealed,[2] the predominant focus of work in the area has been directed at the "first-order" chemistry—the preparation of the metallaboranes themselves and the examination of their structural behavior, their NMR properties, and their intrinsic molecular properties such as fluxionality. By contrast, the reaction chemistry of the metallaboranes, i.e., the "second order" chemistry of the metallaboranes, is relatively only sparsely examined, even though the redox flexibility of the clusters allied with the redox flexibility of many metal centers, particularly those of the transition elements, promises much interest.

In attempts to address this area, we have, often in a preliminary fashion so far, been able to study a few reactions of *arachno*-4-metallanonaboranes[3,4] and *nido*-6-metalladecaboranes,[5] but the general area is, however, still undeveloped.[3−5] In this context, this paper now describes the small-scale examination of the incorporation of the substituted alkyne, 2-methylbut-1-en-3-yne, into *arachno* nine-vertex $[(CO)(PMe_3)_2HIrB_8H_{12}]$ (**1**) and also thereby provides some evidence for the mode of incorporation of acetylene itself into this particular metallaborane, a study on which we recently reported.[3]

Experimental Section

General. Solvents used were reagent grade and dried before use. Reactions were carried out on a standard Schlenk line, and the products were isolated in air using thin-layer chromatography (TLC) on 20 × 20 cm glass plates coated with 0.1 cm of silica gel (Merck, 60 GF_{254}) made from aqueous slurries followed by drying in air at 80 °C. *Arachno* nine-vertex $[(CO)(PMe_3)_2HIrB_8H_{12}]$ (**1**) was prepared according to the literature method.[6] NMR studies were carried out at 5.9 and 11.8 T (fields corresponding to 250 and 500 MHz ^1H frequencies, respectively) using Bruker ARX-250 and AMX-500 spectrometers. Chemical shifts δ are given in ppm to high frequency (low field) of Ξ 100 MHz ($SiMe_4$) for ^1H (quoted ±0.05 ppm), Ξ 40.480 730 MHz (nominally 85% H_3PO_4) for ^{31}P (quoted ±0.5 ppm), and Ξ 32.083 971 MHz (nominally F_3BOEt_2 in $CDCl_3$) for ^{11}B (quoted ±0.5 ppm), Ξ being defined as in ref 7. The chemical shifts were calibrated using solvent deuteron or residual proton resonances as internal secondary standards. Infrared spectra were measured on a Perkin-Elmer Series 1600 FT-IR using 3M Teflon infrared cards.

[†] University of Leeds.

[‡] University of Missouri−St. Louis.

(1) Kennedy, J. D. *Prog. Inorg. Chem.* **1984**, *32*, 519−679. (b) Kennedy, J. D. *Prog. Inorg. Chem.* **1986**, *36*, 211−434. (c) Gilbert, K. B.; Boocock, S. K.; Shore, S. G. In *Comprehensive Organometallic Chemistry*; Wilkinson, G., Abel, E. W., Stone, F. G. A., Eds.; Pergamon: New York, 1982; Part 6, Chapter 41, pp 879−945. (d) Grimes, R. N. In *Comprehensive Organometallic Chemistry*; Wilkinson, G., Abel, E. W., Stone, F. G. A., Eds.; Pergamon: New York, 1982; Part 1, Chapter 5.5, pp 459−453. (e) Barton, L.; Srivastava, S. K. In *Comprehensive Organometallic Chemistry II*; Wilkinson, G., Abel, E. W., Stone, F. G. A., Eds.; Pergamon: New York, 1995; Vol. 1, Chapter 8, pp 275−373. (f) Grimes, R. N. In *Comprehensive Organometallic Chemistry II*; Wilkinson, G., Abel, E. W., Stone, F. G. A., Eds.; Pergamon: New York, 1995; Vol. 1, Chapter 9, pp 374−431. (g) Grimes, R. N. *Chem. Rev.* **1992**, *92*, 251. (h) Saxena, A. K.; Hosmane, N. S. *Chem. Rev.* **1993**, *93*, 1081.

(2) Kennedy, J. D. Disobedient Skeletons; In *The Borane Carborane Carbocation Continuum*; Casanova, J., Ed.; Wiley: New York, 1998.

(3) Bould, J.; Rath, N. P.; Barton, L. *Organometallics* **1996,** *15*, 4916.

(4) For example, see: (a) Boocock, S. K.; Greenwood, N. N.; Hails, M. J.; Kennedy, J. D.; McDonald, W. S. *J. Chem. Soc., Dalton Trans.* **1981**, 1415. (b) Beckett, M. A.; Crook, J. E.; Greenwood, N. N.; Kennedy, J. D.; McDonald, W. S. *J. Chem. Soc., Chem Commun.* **1982**, 552. (c) Beckett, M. A.; Crook, J. E.; Greenwood, N. N.; Kennedy, J. D.; McDonald, W. S. *J. Chem. Soc., Chem Commun.* **1983**, 1228. (d) Bould, J.; Greenwood, N. N.; Kennedy, J. D. *J. Chem. Soc., Dalton Trans.* **1984**, 2477. (e) Beckett, M. A.; Crook, J. E.; Greenwood, N. N.; Kennedy, J. D. *J. Chem. Soc., Dalton Trans.* **1986**, 1879. (f) Beckett, M. A.; Greenwood, N. N.; Kennedy, J. D.; Salter, P. A.; Thornton-Pett, M. *J. Chem. Soc., Chem. Commun.* **1986**, 556. (g) Bunkhall, S. R.; Fontaine, X. L. R.; Greenwood, N. N.; Kennedy, J. D.; Thornton-Pett, M. *J. Chem. Soc., Dalton Trans* **1990**, 73.

(5) For example, see: (a) Bould, J.; Crook, J. E.; Greenwood, N. N.; Kennedy, J. D.; McDonald, W. S. *J. Chem. Soc., Chem. Commun.* **1983**, 949. (b) Bould, J.; Crook, J. E.; Greenwood, N. N.; Kennedy, J. D.; Thornton-Pett, M. *J. Chem. Soc., Dalton Trans.* **1990**, 1441. (c) Ditzel, E. J.; Fontaine, X. L. R.; Greenwood, N. N.; Kennedy, J. D.; Thornton-Pett, M. *J. Chem. Soc., Chem. Commun.* **1989**, 1262. (d) Ditzel, E. J.; Fontaine, X. L. R.; Greenwood, N. N.; Kennedy, J. D.; Sisan, Z.; Thornton-Pett, M. *J. Chem. Soc., Chem. Commun.* **1989**, 1762. (e) Ditzel, E. J.; Fontaine, X. L. R.; Greenwood, N. N.; Kennedy, J. D.; Sisan, Z.; Štíbr, B.; Thornton-Pett, M. *J. Chem. Soc., Chem. Commun.* **1990**, 1741.

(6) Bould, J.; Crook, J. E.; Greenwood, N. N.; Kennedy, J. D.; McDonald, W. S. *J. Chem. Soc., Chem. Commun.*, **1982**, 346. (b) Bould, J.; Crook, J. E.; Greenwood, N. N.; Kennedy, J. D. *J. Chem. Soc., Dalton Trans.* **1984**, 1903.

(7) McFarlane, W. *Proc. R. Soc. London, Ser. A* **1986**, *A306*, 185.

S0276-7333(97)00664-X CCC: $15.00
Publication on Web 02/13/1998

Table 1. Crystal Data and Structure Refinement for Compounds 2 and 3

compound no.	**2**	**3**
empirical formula	$C_{12}H_{33}B_8IrOP_2$	$C_{12}H_{35}B_8IrOP_2$
fw	534.00	536.02
temp/K	193(2)	183(2)
cryst syst	orthorhombic	monoclinic
space group	*Pbca*	$P2_1/c$
a/Å	13.3600(10)	16.08920(10)
b/Å	10.7029(2)	10.04480(10)
c/Å	30.1704(4)	28.04270(10)
β/deg		90.2600(10)
V/Å^{-3}	4307.01(10)	4532.01(6)
Z	8	8
D (calcd)/Mg/m^3	1.647	1.571
abs coeff/mm^{-1}	6.346	6.031
cryst size/mm	0.44 × 0.33 × 0.06	0.5 × 0.3 × 0.3
F(000)	2080	2096
θ range for data collcn/deg	1.35−31.00	1.27−30.00
index ranges	$-20 \le h \le 19, -15 \le k \le 14, -39 \le l \le 43$	$-23 \le h \le 22, -14 \le k \le 14, -37 \le l \le 40$
no. of reflns collcd	30 087	47 549
no. of indep reflns	6844($R_{int} = 0.0652$)	13 191($R_{int} = 0.0686$)
data/restraints/params	6828/0/349	13080/0/529
goodness-of-fit on F^2	1.042	1.172
final R indices [$I > 2\sigma(I)$]		
R_1	0.0363	0.0427
wR_2	0.0906	0.0872
largest diff peak and hole/e Å^{-3}	3.628 and −2.107	3.058 and −1.930

Synthesis of [7-(C(CH$_3$)CH$_2$)-9,9,9-(CO)(PMe$_3$)$_2$-*nido*-9,7,8-IrC$_2$B$_8$H$_{10}$] (2) and [5,5,5-(CO)(PMe$_3$)$_2$-*μ*-6,7-{CHC(CH$_3$)CH$_2$)}-*nido*-5,6-IrCB$_8$H$_{11}$] (3). [(CO)(PMe$_3$)$_2$HIrB$_8$H$_{12}$] (**1**, 55 mg, 135 μmol) was placed in a Schlenk tube, and the tube was evacuated and repressurized with nitrogen. Against a flow of nitrogen, ca. 2 mL of dry *p*-xylene was syringed in. Residual oxygen was then eliminated via two freeze−thaw cycles. An excess of 3-methyl-1-butyne-3-ene (ca. 0.5 mL, 5 mmol) was condensed into the tube, the vacuum tap closed, and the mixture heated (oil bath at 138 °C) for 45 min. After the mixture was cooled, the xylene was removed under dynamic vacuum and the residual solids redissolved in CH_2Cl_2 (20 mL) and filtered through TLC-grade silica gel. The filtrate was reduced in volume and applied to a preparative TLC plate, which was developed using 70/30 CH_2Cl_2/hexane. Two pale yellow bands, A and B, were observed under UV light at R_F 0.9 and 0.6, respectively. These were removed, extracted with CH_2Cl_2, the solutions evaporated, and the residues then separately chromatographed again in 50/50 Et_2O/hexane. Band B appeared to separate into two very close bands at ca. $R_f = 0.50$ (B1) and 0.52 (B2). Of these, band B2 was carefully removed and, after extraction with CH_2Cl_2, evaporation, and crystallization from CH_2Cl_2/hexane, identified as [7-{C(CH$_3$)CH$_2$}-9,9,9-(CO)(PMe$_3$)$_2$-*nido*-9,7,8-IrC$_2$B$_8$H$_{10}$] (**2**, air-stable colorless crystalline solid, 7 mg, 14 μmol, 10% yield; IR ν(CO) 1995 and ν(BH) 2506 cm^{-1}). The other band B2 contained small amounts of two species which we have been unable to separate chromatographically, but slow diffusion of hexane into a solution of the mixture in CH_2Cl_2 gave small yellow air-stable single crystals of [5,5,5-(CO)(PMe$_3$)$_2$-*μ*-6,7-{CHC(CH$_3$)CH$_2$)}-*nido*-5,6-IrCB$_8$H$_{11}$] (**3**, 0.5 mg, 1 μmol, 0.7% yield). We were unable to obtain the other species from band B1 free of **3**, but ^{11}B NMR spectroscopy on the mixture allowed its tentative identification, as described in the text, as [8-{C(CH$_3$)CH$_2$}-9,9,9-(CO)(PMe$_3$)$_2$- *nido*-9,7,8-IrC$_2$B$_8$H$_{11}$] (**4**) (δ(^{11}B), $CDCl_3$ solution: +10.2, +8.0, −10.8, −11.9, −14.7, −20.2, −22.7, and −28.1). Band A contained small amounts of polyboron species, which we have been unable to characterize successfully.

X-ray Diffraction Analyses. A colorless hexagonal plate crystal of **2** and a yellow rectangular crystal of **3** were mounted on glass fibers in arbitrary orientations. Preliminary examination and data collection were performed using a Siemens SMART CCD detector system single-crystal X-ray diffractometer equipped with a sealed-tube X-ray source (50 kV × 40 mA, graphite-monochromated Mo Kα radiation ($\lambda = 0.710\,73$ Å)]. Preliminary unit-cell constants were determined with a set of 45 narrow-frame scans (0.3° in $\tilde{\omega}$). A total of 1325 frames of intensity data were collected with a frame width of 0.3° in $\tilde{\omega}$ and a counting time of 10 s per frame at a crystal-to-detector distance of 4.91 cm. The double-pass method of scanning was used to exclude noise. Data collection time was 6.5 h. The collected frames were integrated using an orientation matrix determined from the narrow-frame scans. The SMART software package was used for data collection, and SAINT[8a] was used for frame integration. For each compound, analysis of the integrated data did not show any decay. Final cell constants were determined by a global refinement of the x, y, z centroids of 8192 reflections ($\theta < 28.0°$ for **2** and $\theta < 30.0°$ for **3**). Absorption corrections were applied to the data using equivalent reflections (SADABS for **2** and XEMP for **3**).[8b] Crystal data and parameters for intensity-data collection for **2** and **3** are listed in Table 1.

The SHELXTL- PLUS (5.03) software package[8c] was used for structure solutions (by direct methods) and refinement. Full-matrix least-squares refinement was carried out by minimizing $\sum w(F_o^2 - F_c^2)^2$. In both cases, the non-hydrogen atoms were refined anisotropically to convergence. All hydrogen atoms for **2** were located and refined freely. For **3**, the boron-cage hydrogen atoms were located and refined freely, and the remaining hydrogen atoms were treated using riding models (AFIX m3). The structure-refinement parameters are listed in Table 1, and drawings of the molecular structures are shown in Figures 1 and 2. A complete listing of the positional and isotropic displacement coefficients for the hydrogen atoms and anisotropic displacement coefficients for the non-hydrogen atoms, are available as Supporting Information.

Results and Discussion

Heating excess 2-methylbut-1-en-3-yne in xylene with *arachno*-[(CO)(PMe$_3$)$_2$HIrB$_8$H$_{12}$] (**1**) in a sealed tube at 138 °C for 45 min, followed by chromatographic separation of the products, afforded two compounds. The first, isolated in 10% yield (unoptimized; reaction-scale ca.100 μmol), was the colorless crystalline solid [7-{C(CH$_3$)=CH$_2$}-9,9,9-(CO)(PMe$_3$)$_2$-*nido*-9,7,8-IrC$_2$B$_8$H$_{11}$] (**2**),

---

[8] (a) Siemens Analytical X-Ray, Madison, WI, 1995. (b) Sheldrick, G. M. Siemens Analytical X-Ray Division, Madison, WI, 1995. (c) Blessing, R. H. *Acta Crystallogr.* **1995**, *A51*, 33−38.

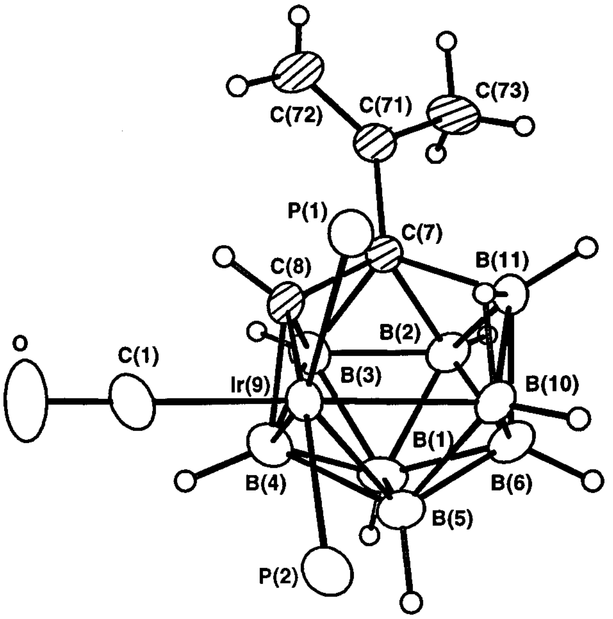

Figure 1. Molecular structure of [7-{C(CH$_3$)CH$_2$}-9,9,9-(CO)(PMe$_3$)$_2$-*nido*-9,7,8-IrC$_2$B$_8$H$_{10}$] (**2**) with the methyl groups on phosphorus omitted for clarity.

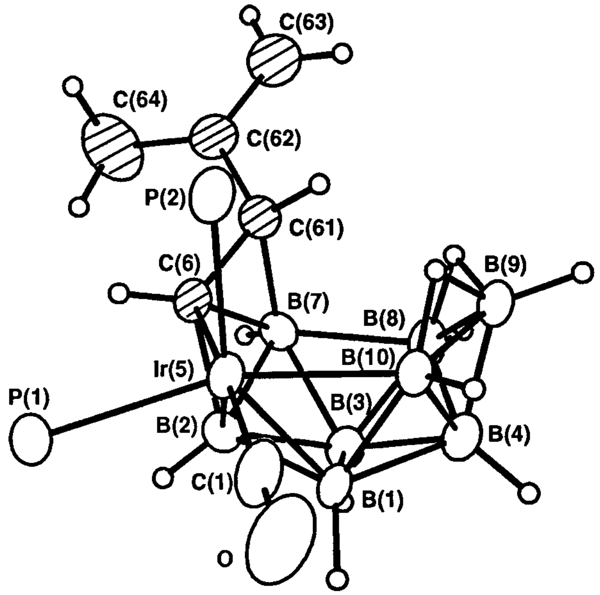

Figure 2. Molecular structure of one of the two unique molecules in the unit cell of [5,5,5-(CO)(PMe$_3$)$_2$-μ-6,7-{CHC-(CH$_3$)CH$_2$}-*nido*-5,6-IrCB$_8$H$_{11}$] (**3**). One hydrogen atom on the methyl group C(64) is obscured, and the methyl groups on phosphorus are omitted for clarity.

Table 2. ^{11}B, ^{1}H, and ^{31}P NMR Data for [7-{C(CH$_3$)CH$_2$}-9,9,9-(PMe$_3$)$_2$(CO)-*nido*-9,7,8-IrC$_2$B$_8$H$_{10}$] (2) in CDCl$_3$ Solution at 300 K[a,b]

assignment	$\delta(^{11}B)$		$\delta(^1H)$	
2	+12.9		+5.15	
5	+8.2	[+6.0][f]	+3.50[c]	[+3.90]
4	−11.7[f]	[−8.8]	+2.55	[+1.96]
11	−12.3		+2.40	
3	−14.7		+2.13	
10	−19.9		+0.62	[+1.02]
6	−22.5		+1.73	
1	−27.5		+1.59	
H(10,11)			−4.27	[−3.57]
H(8)			+3.42	[+2.80]
CH$_2$			+4.71[d]	[+4.57]
CH$_3$			+1.83	[+1.50]
P(CH$_3$)			+1.87[e]	[+1.84][e]
			+1.69[e]	[+1.64][e]

[a] Values in brackets refer to the minor rotamer component (see text) where resolved from the major rotamer component (unbracketed); relative rotamer incidence *ca.* 2:1. [b] ^{31}P NMR $\delta(^{31}P)$ (CD$_3$C$_6$D$_5$, 208 K): major component −40.0 and −40.7, both singlets in ^{31}P−{^{1}H} spectrum; minor component −37.6 and −49.3 (^2J (^{31}P−^{31}P) *ca.* 18.5 Hz). [c] Doublet, J = 15 Hz, probably due to coupling to ^{31}P. [d] Two doublets, AB pattern, $^2J(^1H{-}^1H)$ *ca.* 1.3 Hz, $\Delta\delta$ *ca.* 0.01 ppm. [e] Doublets $^2J(^{31}P{-}^1H)$ 9.3[7.8] and 10.6[9.1] Hz, respectively.[b] [f] Relative intensities of resonances *ca.* 2:[1].[b]

Table 3. Interatomic Distances (Å) and Angles (deg) for Compound 2, with Esd's in Parentheses

Ir(9)−P(2)	2.3278(11)	Ir(9)−P(1)	2.3456(11)
Ir(9)−B(4)	2.220(5)	Ir(9)−B(5)	2.235(5)
Ir(9)−B(10)	2.257(5)	Ir(9)−C(8)	2.192(4)
B(10)−B(11)	1.878(7)	B(11)−C(7)	1.685(5)
C(7)−C(8)	1.541(6)	C(7)−C(71)	1.502(5)
C(71)−C(72)	1.330(6)	C(71)−C(73)	1.494(6)
C(1)−Ir(9)−C(8)	93.8(2)	C(1)−Ir(9)−B(4)	90.0(2)
C(1)−Ir(9)−B(10)	174.5(2)	C(8)−Ir(9)−B(10)	82.2(2)
C(1)−Ir(9)−P(2)	88.57(13)	C(8)−Ir(9)−P(2)	162.21(11)
B(4)−Ir(9)−P(2)	116.62(14)	B(5)−Ir(9)−P(2)	85.89(12)
B(10)−Ir(9)−P(2)	94.12(12)	C(1)−Ir(9)−P(1)	94.85(14)
C(8)−Ir(9)−P(1)	99.47(11)	B(4)−Ir(9)−P(1)	145.27(14)
B(10)−Ir(9)−P(1)	89.56(12)	P(2)−Ir(9)−P(1)	97.89(4)
C(71)−C(7)−C(8)	119.4(3)	C(71)−C(7)−B(11)	118.4(3)
C(8)−C(7)−B(11)	112.2(3)	C(7)−C(8)−Ir(9)	122.8(2)
C(72)−C(71)−C(7)	122.8(4)	C(73)−C(71)−C(7)	117.3(4)

characterized by NMR spectroscopy (Table 2) and by a single-crystal *X*-ray diffraction study. A simple stoichiometric reaction can be written as in eq 1. The

$$[(CO)(PMe_3)_2HIrB_8H_{12}] + HC{\equiv}CC(CH_3){=}CH_2 \rightarrow [(CO)(PMe_3)_2IrC_2B_8H_{10}\{C(CH_3)CH_2\}] + 2H_2 \quad (1)$$

structure of **2** is represented in Figure 1, and selected geometrical dimensions are listed in Table 3. The measured NMR data as well as the detailed interatomic structural dimensions are similar to those recently reported for the unsubstituted analogue [9,9,9-(CO)-(PMe$_3$)$_2$-*nido*-9,7,8-IrC$_2$B$_8$H$_{11}$] (**5**), which is produced in a similar manner in yields of up to 50% from the passage of acetylene gas through solutions of **1** in refluxing xylene.[3] The cluster structure of **2** is also very similar to that of [9,9-(PPh$_3$)$_2$-9,7,8-RhC$_2$B$_8$H$_{11}$] formed in the reaction of [RhCl(PPh$_3$)$_3$] with the [*nido*-5,6-C$_2$B$_8$H$_{11}$]$^-$ anion.[9] It is observed that there is a substituent isopropenyl group on C(7), viz. on the carbon atom in the open face of the cage in the more distal position β to the Ir atom. This positioning could relate to the mode of incorporation of acetylene into the cluster, as mentioned below. The geometry of this isopropenyl substituent is not exceptional; in particular, the geometry about carbon atom C(71) appears to be consistent with sp^3 hybridization, with the C−C−C angles in the range 117−123°.

As noted previously for the unsubstituted analogue **5**,[3] NMR spectra for **2** at room temperature are consistent with the presence of two closely related species, in an approximately 2:1 ratio. These are reasonably postulated as individual rotamers that differ by a twist

---

(9) Jung, C. W.; Hawthorne, M. F. *J. Am. Chem. Soc.* **1980**, *102*, 3024. (b) Lu, P.; Knobler, C. B.; Hawthorne, M. F. *Acta Crystallogr.* **1984**, *C40*, 1704.

contrarotation of the $\{Ir(CO)(PMe_3)_2\}$ ligand sphere relative to the metallacarborane cage (structure **X**). The spectra do not provide enough information to assign the relative orientation of the ligands in the minor rotamer, but steric considerations suggest that it is related to the conformation in structure **X** but with the carbonyl and the lower phosphine group interchanged. For **2** at higher temperatures, individual pairs of resonances for equivalent individual cluster positions coalesce, demonstrating that the contrarotation is a dynamic process. This type of contrarotational fluxionality is so far best defined for $\{PtB_{10}\}$ species of the *nido* 11-vertex geometry.[10] The pair of resonances for $^{11}B(4)$ was the best resolved, and this gave a coalescence temperature of 353 K at 11.8 T (i.e., in the 160.42 MHz ^{11}B spectrum), giving $\Delta G^{\ddagger}_{353}$ of ca. 69 kJ mol^{-1}, essentially the same as the value $\Delta G^{\ddagger}_{368}$ of ca. 71 kJ mol^{-1} previously estimated for **5**.

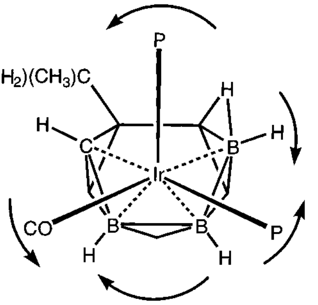

In one experiment, trace amounts of a compound, which from comparison of its ^{11}B NMR spectrum (see Experimental Section) with that of **2** is reasonably suggested to be [8-$\{C(CH_3){=}CH_2\}$-9,9,9-(CO)$(PMe_3)_2$-*nido*-9,7,8-$IrC_2B_8H_{10}$] (**4**), were also observed. The ^{11}B spectrum of this species does not feature resonances attributable to any second rotamer. This perhaps suggests that a steric inhibition arising from the bulk of the pendent isopropenyl group on the α-carbon dictates that only one rotamer is observed. In the chlorinated analogue [9,9,9-(CO)$(PMe_3)_2$-*nido*-9,7,8-$IrC_2B_8H_{10}$-5-Cl)], the presence of a chlorine substituent on vertex B(5) adjacent to the metal produces a similar effect,[3] i.e., only one rotamer is apparent, although Cl is smaller than $\{CHMe_2\}$, so electronic as well as steric effects may also contribute.

Also present in the reaction mixture, but now unequivocally identified by a single-crystal X-ray diffraction study (Figure 2 and Tables 1 and 5) as well as by NMR spectroscopy (Table 4), was the *nido* 10-vertex cluster species [5,5,5-(CO)$(PMe_3)_2$-μ-6,7-$\{CHC(CH_3)CH_2\}$-5,6-$IrCB_8H_{11}$] (**3**). This compound was isolated in trace amounts (<ca. 1% yield according to the stoichiometry of eq 2), although integrated ^{11}B NMR spectroscopy suggested somewhat higher yields, on the order of ca. 2%, in the reaction product mixture. The unit cell of **3** contains two unique molecules; one of these is shown in Figure 2. The configuration of the other is very similar, the only differences, that exceed error limits, are those associated with the phosphine ligands and they are very small. Selected structural dimensions are given in Table 5. The cluster is observed to be based on the conventional *nido*-decaboranyl structural motif,[11] with the $\{Ir(CO)(PMe_3)_2\}$ and {CH} moieties, respectively, occupying the 5- and 6-positions and the pendent propenyl group spanning the C(6)−B(7) edge. In keeping with the *nido* structural descriptor, the B(7)−B(8) distance at 1.950(9) Å is the longest interboron separation, as characteristically found in other *nido* metalladecaboranes[1,4b,12] and in *nido* decaboranes in general.[13]

$$[(CO)(PMe_3)_2HIrB_8H_{12}] + HC{\equiv}CC(CH_3){=}CH_2 \rightarrow [(CO)(PMe_3)_2IrCB_8H_{11}\{CHC(CH_3)CH_2\}] + H_2 \quad (2)$$

Table 4. ^{11}B, ^{1}H, and $^{31}P^{a}$ NMR Data for [5,5,5-(CO)$(PMe_3)_2$-μ-6,7-$\{CH(CH_3)CH_2\}$-*nido*-5,6-$IrCB_8H_{11}$] (3) in $CD_3C_6D_6$ Solution at 300 K

assignment[b]	$\delta(^{11}B)$	$\delta(^{1}H)$
1	+29.6	+5.59
2	+14.1	+4.99
3	+3.2	+5.14
7	−34.2	−0.15
8, 9, 10	−6.6	+3.02
	−7.9(2)	+2.93, +2.85
4	−37.0	+0.63
H(8,9) (9,10)		−3.77(2)
$P(CH_3)$[c]		+1.69, +1.63
CH		*d*
CH_2		+4.59, +4.44
CH_3		*d*

[a] ^{31}P NMR data: $\delta(^{31}P)$ (C_7D_8, 208 K) −44.6 and −53.4; both singlets with $\{^1H\}$ decoupling. [b] Assignments based on $^1H\{^{11}B\}$ selective decoupling and $^{11}B-^{11}B$ COSY experiments. [c] Doublets; $^2J(^{31}P-^1H)$ = 9.0 and 10.0 Hz, respectively. [d] Obscured by PMe_3 and solvent resonances.

Table 5. Interatomic Distances (Å) and Angles (deg) for Compound 3, with Esd's in Parentheses

Ir(5)−P(1)	2.3710(14)	Ir(5)−P(2)	2.345(2)
Ir(5)−B(2)	2.219(6)	Ir(5)−B(10)	2.254(6)
Ir(5)−C(6)	2.162(5)	B(1)−B(10)	1.874(8)
B(2)−C(6)	1.692(8)	B(2)−B(7)	1.897(8)
B(3)−B(7)	1.790(8)	B(7)−C(61)	1.675(8)
B(7)−C(6)	1.826(7)	B(7)−B(8)	1.950(9)
C(6)−C(61)	1.495(7)	C(61)−C(62)	1.498(7)
C(62)−C(63)	1.359(9)	C(62)−C(64)	1.443(10)
C(6)−Ir(5)−B(1)	85.5(2)	C(6)−Ir(5)−B(2)	45.4(2)
B(1)−Ir(5)−B(2)	47.7(2)	C(1)−Ir(5)−B(10)	84.2(2)
C(6)−Ir(5)−B(10)	95.1(2)	B(1)−Ir(5)−B(10)	49.6(2)
C(6)−Ir(5)−P(2)	92.55(14)	B(2)−Ir(5)−B(10)	85.3(2)
B(1)−Ir(5)−P(2)	145.4(2)	B(2)−Ir(5)−P(2)	137.7(2)
B(10)−Ir(5)−P(2)	96.4(2)	C(6)−Ir(5)−P(1)	90.78(14)
B(1)−Ir(5)−P(1)	115.0(2)	B(2)−Ir(5)−P(1)	87.4(2)
B(10)−Ir(5)−P(1)	162.7(2)	P(2)−Ir(5)−P(1)	99.55(5)
C(61)−B(7)−B(3)	133.3(4)	C(61)−B(7)−C(6)	50.3(3)
B(3)−B(7)−C(6)	105.8(4)	C(61)−B(7)−B(2)	102.3(4)
C(61)−C(6)−B(7)	59.6(3)	C(61)−C(6)−B(2)	121.7(4)
B(2)−C(6)−B(7)	65.1(3)	C(61)−C(6)−B(2)	121.7(4)
C(61)−C(6)−Ir(5)	123.8(3)	B(2)−C(6)−Ir(5)	69.1(3)
C(6)−C(61)−B(7)	70.1(3)	C(6)−C(61)−C(62)	121.8(5)
B(7)−C(6)−Ir(5)	118.3(3)	C(63)−C(62)−C(64)	121.1(6)
C(64)−C(62)−C(61)	121.0(6)	C(63)−C(62)−C(61)	117.8(6)

The one-carbon bridge spanning the C(6)−B(7) edge is interesting and novel. A non-hydrogen atom bridging a *nido*-decaboranyl B(5)−B(6) position (equivalent to the

---

[10] Boocock, S. K.; Greenwood, N. N.; Kennedy, J. D.; McDonald, W. S.; Staves, J. *J. Chem. Soc., Dalton Trans.* **1981**, 2573. (b) Crook, J. E.; Greenwood, N. N.; Kennedy, J. D.; McDonald, W. S. *J. Chem. Soc., Dalton Trans.* **1984**, 2487.

[11] Williams, R. E. *Adv. Inorg. Chem. Radiochem.* **1976**, *18*, 67. (b) Wade, K. *Adv. Inorg. Chem. Radiochem.* **1976**, *18*, 60. (c) Rudolph, R. W. *Acc. Chem. Res.* **1976**, *9*, 446.

[12] Reference 1b, p 340.

formally numbered bridged 6, 7 position in **3**) is well recognized, but within this context, there appears to be a substantial variation in the observed bonding behavior, as judged by the variations in the bridged interboron distances. The incorporation of a heteroatom bridge often produces a lengthening in the intervertex separation, and in accord with this, the C(6)−B(7) distance of 1.826(7) Å in **3** is somewhat longer, by about 0.10−0.15 Å, than the other carbon−boron distances in both species **2** and **5** (1.685(5)−1.738(6) Å). We can find no bridged boron−carbon distances for comparison, although there is a proposed hydrogen-bridged carbon−boron linkage of 1.855(14) Å in [(η^6-C_6Me_6)RuN(Me)-CB_9H_{12}(OMe)].[5e] The boron−boron distances in related species that have a main-group element bridging the B(5)−B(6) linkage in a decaborane(14) analogue are 2.69(2) Å in [$B_{10}H_{13}$(μ-PPh_2)],[14] 2.077(2) Å in [$B_{10}H_{12}$-(N_3)(μ-NH_2)],[15] 2.211(5) Å in [(η^5-C_5Me_5)RhB_9H_{12}(μ-NEt_2)],[16] 1.872 Å in [$B_{10}H_{12}$-μ-PHC(^{ter}Bu)$B_{10}H_{12}$(SMe_2)],[17] and 1.864(4) Å in the [$OB_{18}H_{21}$]$^-$ anion.[18] In the phosphorus-bridged 11-vertex monocarborane [(μ-PPh)-$B_{10}H_{10}$CNMe$_3$], the bridged interboron distance is 1.839-(7) Å,[19] and in its carbon-bridged anionic analogues [(μ-CHPh)$B_{10}H_{10}$CPh]$^-$ [20a] and [(μ-CHMe)$B_{10}H_{10}$CMe]$^-$,[20b] the distances are 1.86(2) and 1.847(2) Å, respectively. In the smaller clusters [(μ-NH^{ter}Bu)B_5H_{10}][21a] and [μ-(PPh_2)B_5H_7{CpFe(CO)$_2$}],[21b] the bridged interboron distances are 2.080(4) and 2.683(5) Å, respectively. The BHB interboron distance in $B_{10}H_{14}$ itself is 1.776(5) Å, with other $B_{10}H_{14}$ interboron distances, apart from the long B(5)−B(10)/B(7)B(8) one mentioned above, averaging at ca. 1.74 Å.[13] In the gold-bridged compound [5,6-μ-($AuPR_3$)-*nido*-$B_{10}H_{13}$], this distance appears to be somewhat shorter than in $B_{10}H_{14}$ itself, 1.745(22) Å.[22]

Except for the small cages involving N and P bridges, these data are inconsistent with the atom size of the bridging heteroatom. In [$B_{10}H_{13}$(PPh_2)], the distance of 2.69(2) Å is clearly nonbonding and it is reasonable to postulate two boron−phosphorus two-electron, two-center bonds in a four-electron bridge.[14] The same can be said for [(μ-NH^{ter}Bu)B_5H_{10}] and [μ-(PPh_2)B_5H_7{CpFe-(CO)$_2$}]. The distance in the latter, 2.683(5) Å,[21b] compares well with that for [$B_{10}H_{13}$(PPh_2)]. At the other extreme, the short interboron distances for the B−H−B link in $B_{10}H_{14}$ and for the B−Au−B link in [($AuPR_3$)-$B_{10}H_{13}$] are generally taken as indicative of three-center, two-electron bonds and, thus, have normal deltahedral interboron values. Carbon-bridged species are more ambiguous. In **3**, the carbon-bridged C(6)−B(7) distance of 1.826(4) Å is somewhat longer than typical intracluster deltahedral boron−carbon distances of ca. 1.65−1.70 Å, but nevertheless, it is short enough to imply a substantial direct bonding interaction. The cluster-to-bridge intercarbon distance C(6)−C(61) at 1.495(7) Å indicates a strong two-electron, two-center intercarbon single bond, and the distance between C(61) and sp^2-hybridized C(62) is 1.498(7), which is consistent with a C(sp^2)−C(sp^3) linkage; however, the angle C(6)−C(61)−B(7) of 70.1(3)° argues against two two-electron, two-center bonds from an sp^3-hybridized C(61) to C(6) and B(7), as this angle would be too acute for the implied sp^3-hybridized carbon. On the other hand, electron-precise cyclopropane, formally with three two-electron, two-center bonds holding its three cluster atoms together, has 60° angles and an intercarbon distance of 1.52 Å, marginally shorter than the typical sp^3−sp^3 intercarbon distance of 1.534 Å. In **3**, the other arm of the bridge B(7)−C(61) at 1.675 (8) Å is within a typical carbon−boron deltahedral range, however, so a useful working picture of the bonding could involve a C(6)−C(61) bond order of more than two, involving both a C(6)−C(61) bond of two-electron, two-center character and a C(6)−C(61)-B(7) bond of two-electron, three-center character. The bonding mode is clearly of interest and might merit suitable molecular-orbital studies. The only example of what appears to be a B−C−B three-center, two-electron bond involving a carbon bridge appears in *nido*-4,5-[FeCp(CO)(PPh_3)(η^1:μ-*trans*-Me-C═CMe]-2,3-$Et_2C_2B_4H_5$.[23] In this case, the bridged B−B distance is 1.84(2) Å, again not significantly different from distances involving two two-center, two-electron bonds. In this general area it is noted that NMR data suggest[24] that one of the isomers of the tetracarbon carborane $Me_4C_4B_7H_9$ has a [μ-6,7-(CHMe)-5,6,10-Me_3-5,6,10-$C_3B_7H_8$] configuration, which would somewhat resemble the structure of compound **3**, with a bridging {CHMe} moiety spanning the equivalent carbon−boron edge. Unfortunately, structural work on this particular tetracarbon carborane isomer has not been reported, thus precluding a direct comparison of this interesting feature.

The alkyne addition is similar to that observed previously[3] for the reaction between unsubstituted C_2H_2 and *arachno*-[(CO)(PMe_3)$_2$HIrB_8H_{12}], where two possible reaction modes were postulated. Both involve an initial facile loss of dihydrogen in an *arachno* → *nido* metallanonaborane step.[6] Hence, one proposed process involved an initial hydroboration of the alkyne by the metallaborane cluster followed by coordination of the pendent alkenyl moiety to a vacant coordination site on iridium. Alternatively, initial coordination of the alkyne to the iridium end of the iridanonaborane cluster together with a concerted hydrogen-atom rearrangement about the open face, followed by insertion of the second carbon atom together with dihydrogen elimination, leads to the metallacarborane. This latter step is now more likely in view of the work reported here. In the case of a substituted alkyne, RC≡CH, the hydroboration step might be expected to feature a normal anti-Markovnikov addition with the substituent group R

---

[13] Tippe A.; Hamilton, W. C. *Inorg. Chem.* **1969**, *8*, 464.

[14] Friedman, L. B.; Perry, S. L. *Inorg. Chem.* **1973**, *12*, 288. (b) Beckett, M. A.; Kennedy, J. D. *J. Chem. Soc., Chem. Commun.* **1983**, 575.

[15] Müller, J.; Paetzold, P.; Boese, R. *Heteroatom Chem.* **1990**, *1*, 461.

[16] Doerfler, U.; Clegg, W.; Kennedy J. D.; Thornton-Pett, M. Manuscript in preparation.

[17] Meyer, F.; Paetzold, P.; Englert, U. *Chem. Ber.* **1994**, *127*, 93.

[18] Jelínek, T.; Kennedy, J. D.; Štíbr, B.; Thornton-Pett, M. *J. Chem. Soc., Chem. Commun.* **1995**, 1665.

[19] Wright, W. F.; Huffman, J. C.; Todd, L. J. *J. Organomet. Chem.* **1978**, *148*, 7.

[20] Tolpin, E. I.; Lipscomb, W. N. *Inorg. Chem.* **1973**, *12*, 2257. (b) Churchill, M. R.; DeBoer, B. G. *Inorg. Chem.* **1973**, *12*, 2674.

[21] Gaines, D. F.; McGaff, R. W.; Powell, D. R. *Inorg. Chem.* **1993**, *32*, 2612. (b) Goudreau, B. H.; Ostrander, R. L.; Spencer, J. T. *Inorg. Chem.* **1991**, *30*, 2066.

[22] Wynd, A. J.; McLennan, A. J.; Reed, D.; Welch, A. J. *J. Chem. Soc., Dalton Trans.* **1987**, 2761. (b) Wynd, A. J.; Welch, A. J.; Parish, R. V. *J. Chem. Soc., Dalton Trans.* **1990**, 2185.

[23] Mirabelli, M. G. L.; Carroll, P. J.; Sneddon, L. G. *J. Am. Chem. Soc.* **1989**, *111*, 529.

[24] Finster, D. C.; Grimes, R. N. *J. Am. Chem. Soc.* **1981**, *103*, 2675.

found on the carbon atom adjacent (α) to the metal atom in the product. On the other hand, in the alternative path, initial coordination of the unsubstituted end of the alkyne to the vacant metal coordination site would result in the R group being found on the carbon-atom position β to the metal center. For the reaction with the enyne reported herein, the major product **2** is clearly consistent with the latter reaction path, although, as mentioned above, a trace amount of what was probably the α-substituted species **4** was detected in one experiment. Compound **3** would appear to represent incomplete incorporation of the enyne moiety into the cluster framework. In principle, **3** relates to **2** by the incorporation of the *exo*-cluster bridging carbon atom into the *nido* 10-vertex $\{IrCB_8\}$ cage to form an 11-vertex $\{IrC_2B_8\}$ cluster species. However, species **3** may not be a direct precursor to **2**; rather, an initial complex may form between the enyne and **1** and then rearrange in either of two modes to give **2** or **3**.

The nine-vertex iridanonaborane system is remarkably versatile. The results described herein clearly extend the range of heteroatom species that can be incorporated into the nine-vertex $\{IrB_8\}$ matrix. Thus far it has been possible to incorporate two carbon atoms from alkynes to form *nido* 11-vertex $[(CO)(PMe_3)_2IrC_2B_8H_{11}]$[3] and *nido* 11-vertex $[(CO)(PMe_3)_2IrC_2B_8H_{11}(C_6H_{11})]$,[3] one sulfur atom via H_2S to form *nido* 10-vertex $[(PMe_3)_2HIrSB_8H_{10}]$ and *closo* 10-vertex $[(PMe_3)_2HIrSB_8H_8]$, two sulfur atoms, also via H_2S, to give *nido* 11-vertex $[(PMe_3)_2HIrS_2B_8H_8]$,[3] another mole of $[(CO)(PMe_3)_2IrB_8H_{11}]$ to afford 18-vertex $[(CO)(PMe_3)_2IrB_{16}H_{14}Ir(CO)(PMe_3)_2]$,[25] *nido*-$B_{10}H_{14}$ to afford $[(CO)(PMe_3)_2IrB_{17}H_{20}]$,[26] and both $B_{10}H_{14}$ and another mole of $[(CO)(PMe_3)_2IrB_8H_{11}]$ to afford the large 28-vertex cluster compound $[(PMe_3)_2IrB_{26}H_{24}Ir(CO)(PMe_3)_2]$.[27] In addition, the transition metal moiety $[Pt(PMe_3)_2]$ has been inserted into the cluster to afford *arachno*-$[(PMe_3)_2(CO)(H)IrB_8H_{10}Pt(PMe_3)_2]$.[4d] The present work extends carbon-atom incorporation to enynes to give *nido* 10-vertex $[(CO)(PMe_3)_2\text{-}\mu\text{-}\{(6,7)\text{-}CHC(CH_3)CH_2\}\text{-}5,6\text{-}IrCB_8H_{11}]$ (**3**) via the incorporation of just one carbon atom, as well as additional examples of *nido* 11-vertex clusters such as 11-vertex $[(CO)(PMe_3)_2IrC_2\{C(CH_3)CH_2\}B_8H_{10}]$ (**2**) by the incorporation of two carbon atoms. Clearly there is much further potential for additional “second order” reaction chemistry from this and related metallaboranes, and we continue to explore this fascinating area.

Acknowledgment. We thank the Johnson-Matthey Company for a loan of $IrCl_3.3H_2O$, the National Science Foundation, the EPSRC (U.K.), the Petroleum Research Fund of the American Chemical Society, the Missouri Research Board, and UM−St. Louis for financial support of this work, and the NSF and the UMSL Center for Molecular Electronics for equipment grants. We thank Dr. J. Braddock-Wilking and Simon Barrett for assistance with NMR spectra.

Supporting Information Available: Tables of crystal data and structure refinement, atomic coordinates, interatomic distances, anisotropic displacement parameters, and hydrogen coordinates for **2** and **3** (14 pages). Ordering information is given on any current masthead page.

OM970664Q

---

(25) Barton, L.; Bould, J.; Kennedy, J. D.; Rath, N. P. *J Chem. Soc., Dalton Trans.* **1996**, 3145.

(26) Bould, J.; Clegg, W.; Kennedy, J. D.; Teat, S. J.; Thornton-Pett, M. *J Chem. Soc., Dalton Trans.* **1997**, 2005.

(27) Bould, J.; Kennedy, J. D.; Barton, L.; Rath. N. P. *Chem. Commun.* **1997**, 2405.